RAA 2015 Vol. **15** No. **3**, 443–452 doi: 10.1088/1674–4527/15/3/011
http://www.raa-journal.org *http://www.iop.org/journals/raa*

Research in Astronomy and Astrophysics

Simulations of ultra-long wavelength interferometers in Earth orbit and on the lunar surface

Mo Zhang[1], Mao-Hai Huang[1] and Yi-Hua Yan[2]

[1] Key Laboratory of Space Astronomy and Technology, National Astronomical Observatories, Chinese Academy of Sciences, Beijing 100012, China; *mhuang@nao.cas.cn*
[2] Key Laboratory of Solar Activity, National Astronomical Observatories, Chinese Academy of Sciences, Beijing 100012, China

Received 2013 December 4; accepted 2014 June 21

Abstract We present simulations of interferometers in Earth orbit and on the lunar surface to guide the design and optimization of space-based ultra-long wavelength missions, such as those pioneered by China's Chang'e Program. We choose parameters and present simulations using simulated data to identify inter-dependencies and constraints on science and engineering parameters. A regolith model is created for the lunar surface array simulation, and the results show that the lunar regolith will have an undesirable effect on the observations. We estimate data transmission requirements, calculate sensitivities for both cases, and discuss the trade-off between brightness temperature sensitivity and angular resolution for the Earth orbit array case.

Key words: techniques: interferometric — Moon — methods: data analysis

1 INTRODUCTION

The ultra-long wavelength (ULW) spectral window in astrophysics is generally defined as the radio band at wavelengths longer than 10 m. In this paper, we emphasize wavelengths between 10 m and 10 km (0.03∼30 MHz). The ULW is a potentially significant frequency range for radio astronomy but currently has not well been explored (Jester & Falcke 2009). Due to observational constraints from Earth's ionosphere and artificial and natural radio frequency interferences, astronomical observations in this frequency range are more readily conducted from space. Antennas deployed in Earth orbit or on the lunar surface (Jester & Falcke 2009) are able to receive signals well below 10 MHz, being mainly limited by the interplanetary plasma cutoff frequency of 20∼30 kHz. Compared with ground-based observations, space interferometers allow for baselines many times longer than the diameter of Earth, making much higher angular resolutions achievable even at ULW bands.

For astronomical space interferometry observations, requirements on array configurations and observation time windows vary greatly, depending on the properties of celestial objects and the nature of the astronomical phenomena being observed. Observations of compact sources require high angular resolution, therefore, long baselines are necessary, but studies of faint extended sources require high surface brightness sensitivities, which demand high array filling factors and therefore shorter baselines are essential. A full-sky survey mission would also impose different requirements compared with a time-domain event monitor.

Science requirements, engineering constraints and environmental obstacles must all be evaluated quantitatively in a trade-off study. Given the highly different, and sometimes contradictory, requirements of astronomical space interferometry missions, the outcome of the mission needs to be evaluated quantitatively against a set of science and engineering requirements and environmental constraints so that trade-offs appropriate to a space ULW mission can be made. Engineering factors to be considered include the accuracy of baseline determination, time synchronization, onboard processing and data transmission capabilities, and, for a lunar surface mission, power supply and antenna deployment. Environmental effects include the effects of space plasma and radio interference. Interplanetary, interstellar and lunar plasma degrade observation results through angular broadening, time-delay and Faraday rotation effects. Artificial and natural ULW radio interference from Earth that escapes the ionosphere is among the main obstacles that need to be overcome for ULW observations conducted near Earth (Woan 2000).

This paper aims to establish a framework for the trade-off study. Specifically, we simulate observations made by an antenna array for two cases: an array deployed in Earth orbit, and an array deployed on the lunar surface. We first select orbital parameters for the Earth orbit case and antenna positions for the lunar surface case and then obtain the (u, v)-coverage for each, then we simulate the signal that the antennas receive and use these to create images. The quality of the synthesized beam is used to evaluate the image quality. We add the number of antennas, orbit, regolith properties, integration time, duty cycle, bandwidth and observing frequency into the simulation and observe how the results of the simulated observations are affected by these factors.

As a first iteration of a trade-off study between scientific requirements and engineering constraints, in this paper we set the requirements for a hypothetical space ULW mission to the values given in Table 1.

Table 1 Mission Requirements

Parameter	Value
Number of antennas	≥ 2
Baseline range:	
– Earth orbit	$20 \sim 14\,000$ km
– Lunar surface	10 km
Angular resolution[a]:	
– At $0.1 \sim 1$ MHz	$\sim 6^\circ$
– At $1 \sim 10$ MHz	$\sim 0.2^\circ$
Beam DM (See Sect. 2.2)	>10
Observing frequency	$0.3 \sim 30$ MHz
Antenna type	Dipole
Number of polarizations	2

Notes: [a] 10 times better than best existing surveys.

In Sections 2 and 3, we present simulations of an antenna array in Earth orbit and on the lunar surface, respectively, and estimate data transmission requirements for both cases; in Section 4, we discuss sensitivities; finally, in Section 5, we give a summary.

2 SIMULATION FOR AN ARRAY IN EARTH ORBIT

2.1 Simulation Parameters

Compared with ground-based antenna arrays, in Earth orbit, an array experiences real-time 3D movements, and the (u, v)-coverage may be significantly different and vary greatly when the synthesized beam is pointing in different directions. In addition, during observations, one or more antennas may be on the backside of the Earth, where the signal from some directions is blocked. In general, a strategy to maximize the number of available antennas at certain observation periods is needed to

Table 2 Array Parameters for the Earth Orbit Simulation

Parameter	Antenna 1	Antenna 2	Antenna 3
Perigee (km)	500	500	700
Apogee (km)	500	700	700
i (°)	0	0	0
ω (°)	0	0	0
Ω	...	...	...
t_0	0	0	0
Duty cycle	1 s per 90 s (see Sect. 2.3)		
Observing frequency	10 MHz		
Phase center	North Celestial Pole		

Table 3 Beam DM for Different Observation Periods

Observation period (h)	Theoretical resolution ($''$)	Beam DM
1	12	14
6	2	31
24	0.7	60

improve the (u, v)-coverage, and therefore the image quality. Below, we examine a relatively simple case in which the source is never occulted by Earth. The simulation parameters are listed in Table 2. All three antennas are sent into a 500 km orbit by one launch. Antenna 2 needs an orbital maneuver and antenna 3 needs two steps of orbital maneuvers to reach the expected orbits.

2.2 Simulation Results

Figures 1, 2 and 3 show the (u, v)-coverages and cross-sectional views of the synthesized beams for integration times of 1 h, 6 h and 24 h, respectively. As shown in the right panels of these figures, the beam directivity improves with longer integrations. The diffraction-limited theoretical resolution and the beam directivity measure (DM), defined as the maximum value of the main beam divided by the root mean square "noise" in the beam map, are shown in Table 3 for different observation periods. Observation quality for sources in other directions can be simulated using the same method, with the effect of Earth occultations considered if necessary.

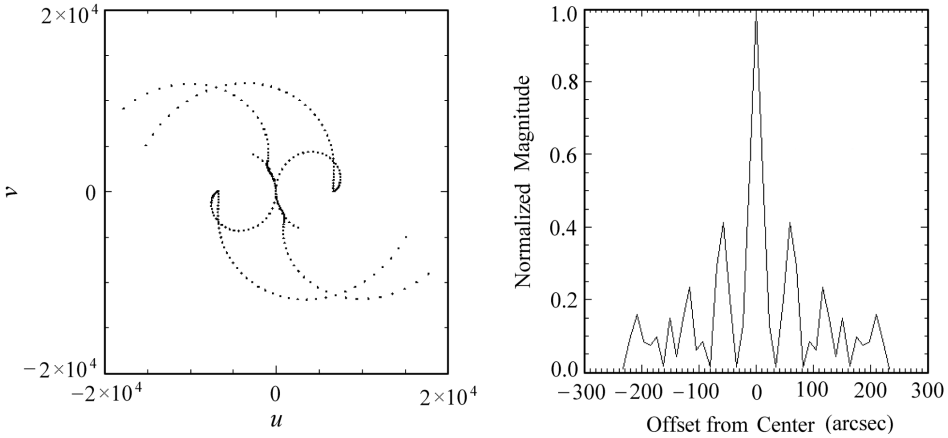

Fig. 1 (u, v)-coverage and beam profile for a 1 h observation.

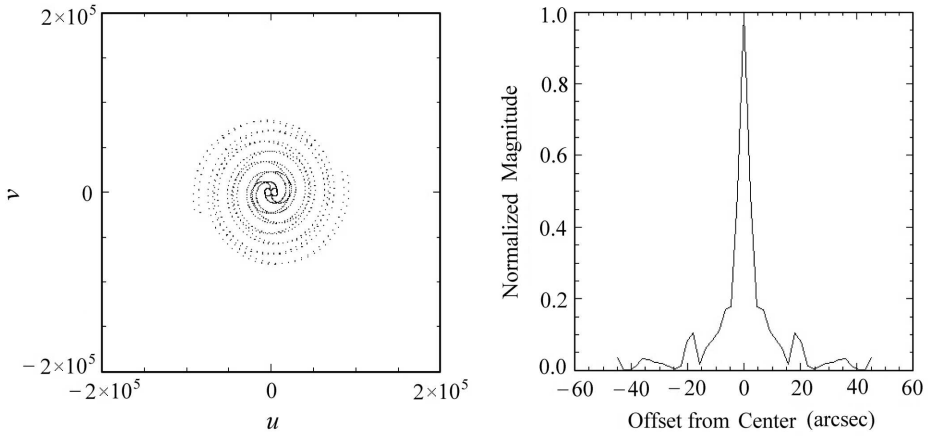

Fig. 2 Same as Fig. 1, but for 6 h.

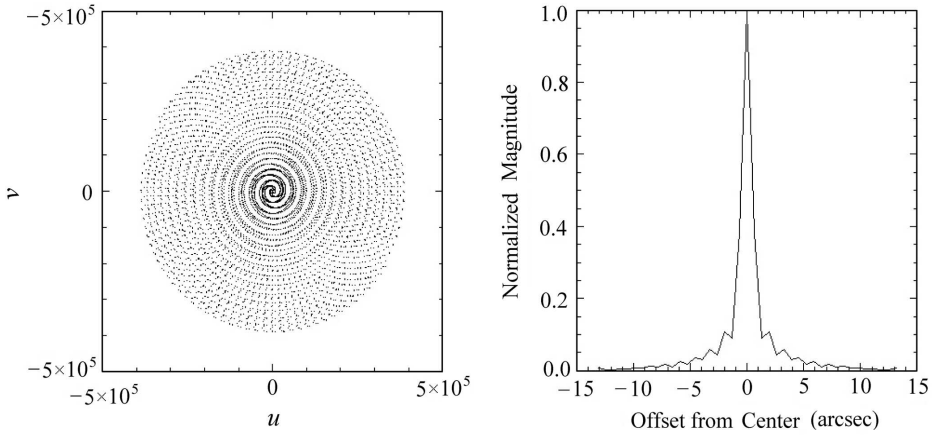

Fig. 3 Same as Fig. 1, but for 24 h.

2.3 Data Transmission Requirements

We assume that the ULW signal received by the antenna is sampled without down-conversion, and all the signals are transmitted to the ground for processing. The data volume is the product of the bits per sample, sampling frequency, integration time and number of polarizations. For an observing frequency of 10 MHz, the sampling frequency must be at least 20 MHz for lossless recovery, according to the Nyquist sampling theorem. We also assume that each sample occupies 1 bit of storage per polarization and that there are two polarizations per antenna, in which case each antenna will achieve a data rate of $10\ \mathrm{MHz} \times 2\ \times 1\,\mathrm{bit\ per\ sample} \times 2\ \mathrm{polarizations} = 40$ Mbps, not including housekeeping and auxiliary data.

We adopt the parameters of a recent study by CNES (Peragin et al. 2012) to evaluate constraints on downlink requirements in the X-band. This study shows that a volume of 39.9 Gb data can be downloaded in the X-band with a 5 m station, considering a 95 min orbit with an 8 min pass window on average and three passes per day. An observation duty cycle is applied to reduce the data volume because the downlink speed is not fast enough if data are taken all the time. As shown in Table 4, if

Table 4 Data Transmission Requirements for the Earth Orbit Array

Parameter	Value
Observing frequency	10 MHz
Sampling frequency	20 MHz
Duty cycle	1 s per 90 s
Bits per sample	1
Number of polarizations	2
Data rate requirement (one station)	27 Mbps

the observation duty cycle is set to 1 s per 90 s, the bandwidth requirement is $\sim$ 27 Mbps per antenna station, which is acceptable.

2.4 Discussion

In our simulations, we assume that the antennas are nearly collocated when the observation starts. This is not generally true. The (u, v)-coverage for an arbitrary initial configuration or an arbitrary period of time, and the statistical properties thereof, can be studied based on the method given in this section.

In the design of some space VLBI missions, the antennas are always parallel to the surface of the Earth. With multiple antennas in different orbit positions, this design will result in nonparallel beams, which in general will reduce sensitivity and (u, v)-coverage. For our simulations above, however, this issue does not exist because the orbital plane is on the equator and the antennas always point to the Celestial North Pole, which is the phase center. In a simulation of a general case, the issue of nonparallel antennas should be considered.

If one needs to make observations with high time resolution, such as of solar radio bursts, the (u, v)-coverage of each snapshot may be very poor, especially when using a small number of antennas. For such cases, further investigation is required to develop mission configurations and data reduction techniques.

3 SIMULATION FOR AN ARRAY ON THE LUNAR SURFACE

3.1 Lunar Regolith Modeling

The relative permittivity of the lunar regolith is approximately 6 (Woan 1996). For a dipole lying on the lunar surface, the response to the signal transmitted from below the lunar surface will be 4.5 times that for a signal from above it (Woan 1996).

The depth of lunar regolith is about 10 m (Lindsay 1976). If the observing frequency is 20 MHz, the signal transmission distance in the regolith is about two times the wavelength, with a travel time of about 100 ns. The signal an antenna receives is the sum of the signals from the sky and from beneath the lunar surface. For the same source, the two signal components are emitted at different times due to reflection of the signal in the lunar regolith. Greater incidence angles result in a longer optical path in the regolith. The regolith will affect the coherence of signals and therefore the imaging quality in complex ways. In the following, we quantitatively show the effect with a simplified model to explain how the lunar regolith affects such observations.

Figure 4 shows a simplified model of the lunar regolith. Below the regolith is bedrock, which serves as a reflector. This model ignores the complex structure of the lunar regolith and bedrock; it assumes that the depth of the regolith is constant, the regolith is uniform and isotropic, and the boundary between regolith and bedrock is flat.

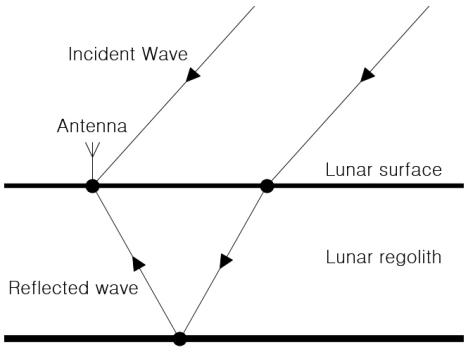

Fig. 4 Simplified signal transmission path model for the lunar regolith.

3.2 Simulation Results

Table 5 shows the parameters we used in the lunar surface simulation, considering there are only two antennas, one on the lander and one on the rover. Both of them are on the near side of the Moon.

Table 5 Array Parameters for the Lunar Surface Simulation

Parameter	Value
Number of antennas	2
Antenna latitude	45° N
Antenna configuration	East-west, 10 km separation
Hour-angle sampling range	$-60^\circ \sim 60^\circ$
Observation wavelength	15 m
Source position	North Celestial Pole
Lunar regolith:	
– Depth	10 m
– Refractive index (Lindsay 1976)	1.5
– Signal attenuation ratio [a]	0.1
Antenna type	Short dipole
Number of samples	100

Notes: [a] Defined as the ratio of the signal magnitude from beneath the lunar surface to that from above, without considering antenna gain.

Table 6 Beam DM for Different Parameters

Lunar regolith	Beam DM
Not considered	17
Taken into account	15

Figures 5 and 6 show the (u, v)-coverage and beam profiles of the simulation. By comparing the two beam profiles in Figure 6, one can see that the beam DM is smaller when the effect of lunar regolith is taken into account (Table 6). We conclude that the lunar regolith will have an undesirable effect on imaging, which confirms the above discussion.

3.3 Data Transmission Requirements

Compared with the Earth orbit antenna array, the data transmission bandwidth for a lunar array is much more limited, approximately 2.5 Mbps in the case of the Chang'e-1 mission. We assume the

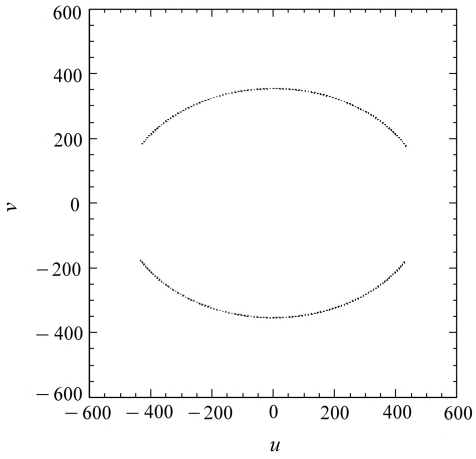

Fig. 5 (u, v)-coverage of the two-antenna array.

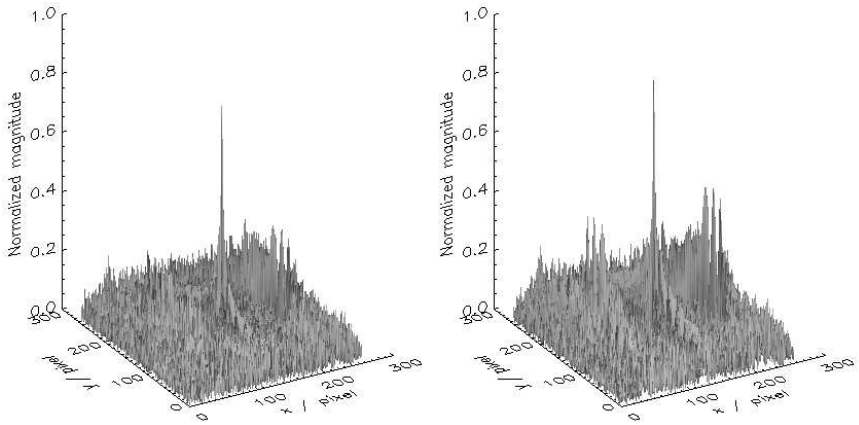

Fig. 6 Normalized beam profile when ignoring the effect of lunar regolith (*left*) and when taking it into account (*right*).

antennas are located on the near side of the Moon and are visible from a ground station for 8 hours a day on average. Furthermore, we assume that each antenna has a dedicated downlink channel with a capacity of 2.5 Mbps, downlinking data 8 hours per day; for an observing frequency of 10 MHz, 1-bit sampling and two polarizations, a duty cycle of 1 s per 48 s is needed to meet the data transmission bandwidth requirement. According to the long-term plan of the Chang'e Program, we assume the lander and the rover are on the near side of the Moon. If they are on the far side of the Moon, a relay satellite orbiting around the Moon is needed. The transmission capability of the relay satellite is assumed to be the same as the lander and the rover, so the calculations are still applicable.

4 ARRAY SENSITIVITY

We assume basic observational parameters to derive the flux sensitivity and brightness temperature sensitivity of the antenna arrays. When the antenna beam is much larger than the angular size of the

Table 7 Flux Sensitivity for Different Array Parameters

Number of antennas	$\lambda = 10$ m (30 MHz)		$\lambda = 30$ m (10 MHz)		$\lambda = 300$ m (1 MHz)	
	Bandwidth (MHz)	Sensitivity (Jy)	Bandwidth (MHz)	Sensitivity (Jy)	Bandwidth (MHz)	Sensitivity (Jy)
2		10		18		43
3	1	6	1	10	0.1	24
10		1		2		6
2		3		5		13
3	10	1	10	3	1	7
10		0.4		0.8		2

Table 8 Temperature Sensitivity for Different Array Parameters

Bandwidth (MHz)	Number of antennas	Temperature sensitivity ($\sigma_{\rm t}$) at $\lambda = 30$ m (K)	
		Earth orbit: $D = 14\,000$ km[a]	Lunar surface: $D = 10$ km
	2	1×10^{12}	6×10^5
1	3	7×10^{11}	3×10^5
	10	2×10^{11}	1×10^5
	2	4×10^{11}	2×10^5
10	3	2×10^{11}	1×10^5
	10	6×10^{10}	3×10^4

Notes: [a] The maximum baseline in this orbit is used for calculation. A shorter baseline results in better temperature sensitivity. See Section 4.

source, the observer is interested in the flux sensitivity; when the beam is comparable to or smaller than the source, the observer is interested in the brightness temperature sensitivity.

The flux sensitivity can be defined as

$$\sigma_{\rm s} = \frac{2kT_{\rm sys}}{A_e\sqrt{n(n-1)\Delta\nu\tau n_{\rm p}}}({\rm Jy})\,, \tag{1}$$

where $T_{\rm sys}$ is the antenna system temperature, n is the number of antennas, $\Delta\nu$ is the bandwidth or channel width, τ is the integration time, $n_{\rm p}$ is the number of polarizations, $A_{\rm e}$ is the effective collecting area of one dipole, which is defined as $3\lambda^2/8\pi$ (Woan 1996), and k is the Boltzmann constant (1380 Jy K^{-1} m^2).

The brightness temperature sensitivity is defined as

$$\sigma_{\rm t} = \frac{D^2T_{\rm sys}}{A_e\sqrt{n(n-1)\Delta\nu\tau n_{\rm p}}}({\rm K})\,, \tag{2}$$

where D is the maximum baseline of the interferometer array.

Tables 7 and 8 show the two types of sensitivity for different observation parameters (bandwidth, observation wavelength and antenna number), assuming $n_{\rm p} = 2$ and τ =86 400 s. A reduction of 36% in the sensitivity caused by 1-bit sampling has been taken into account (Thompson et al. 2001). For ULW observations, $T_{\rm sys}$ is dominated by the Galactic background radio emission; at frequencies above 2 MHz, it can be approximated by a power law (Jester & Falcke 2009)

$$T_{\rm sys} = 16.3 \times 10^6{\rm K}\left(\frac{\nu}{2\ {\rm MHz}}\right)^{-2.53}. \tag{3}$$

At frequencies below 2 MHz, we use the value predicted by the *RAE-2* spacecraft, 2×10^7 K at 1 MHz (Novaco & Brown 1978).

We can then choose array parameters that meet the requirements to observe specific radio sources at a certain level of flux density based on these results. For example, the average flux density of 3C 273 is about 10^2 Jy at 30 MHz, according to the flux densities of active radio sources in the 10 kHz $\sim$ 100 MHz range from the ESA (Bely et al. 1997) design study, adapted from Zarka et al. (1997).

For thermal sources, for example regions of ionized gas surrounding massive stars, the maximum brightness temperature is approximately 2×10^4 K. Optically-thick thermal bremsstrahlung emission dominating the quiet Sun produces brightness temperatures of order 10^6 K (White 2007). For non-thermal sources, the brightness temperature of the Galactic radio background radiation from the polar regions is 2.3×10^7 K at 1 MHz (Cane 1979), and can be as high as 10^{12} K for synchrotron radiation sources (Wilson et al. 2009).

We also note that temperature sensitivity must be high enough to achieve sufficient Signal to Noise Ratio (SNR) :

$$\mathrm{SNR} = \frac{T_{\mathrm{sys}}}{\sigma_{\mathrm{t}}} = \frac{A_e}{D^2}\sqrt{n(n-1)\Delta\nu\tau} = f\sqrt{\Delta\nu\tau}\frac{\sqrt{n(n-1)}}{n}\,, \tag{4}$$

where $f = nA_{\mathrm{e}}/D^2$ is the filling factor of the interferometer. A lunar based observation on the quiet Sun at 10 MHz with 10 antennas, that uses a 90 day observation period, 1 s per 90 s duty cycle, 10 km maximum baseline and a 1 MHz bandwidth will achieve an SNR of 10.

The maximum baseline is the key factor when considering trade-offs between sensitivity and angular resolution. Taking a low Earth orbit array as an example, an observation with 10 antennas that uses a 10 MHz observing frequency, a 10 MHz bandwidth, a 90 day observation period, 1 s per 90 s duty cycle and 14 000 km maximum baseline will achieve a temperature sensitivity of 6×10^{10} K. In such a case, the angular resolution is about $0.5''$, far from being able to resolve synchrotron self-absorbed sources at 10^{12} K. Because noise in brightness temperature (σ_{t}) is proportional to D^{-2} and angular resolution is proportional to D^{-1}, reducing the maximum baseline will allow various kinds of sources to be observable with sufficient temperature sensitivity and angular resolution, such as the Galactic radio background radiation at arcminute resolution and solar bursts. There are multiple methods to limit the maximum baseline for an Earth orbit array, either by choosing observing windows so that data for extended sources are only taken when the antennas are close to each other, or by formation flying.

5 SUMMARY

We demonstrate a simulation framework for ULW space arrays in Earth orbit and on the lunar surface to help the overall system design of future ULW missions. We present simulations, estimate the data transmission requirements and calculate sensitivities for both cases. For the lunar surface array case, we create a simplified regolith model, and the results show that the regolith would have an undesirable effect on the observation. For the Earth orbit array case, we discuss the relation between the maximum array baseline and the angular resolution and the brightness temperature sensitivity to show the trade-off between brightness temperature sensitivity and angular resolution.

Acknowledgements We would like to thank the referee for the useful and valuable comments in revising the manuscript. This work was supported by a civilian space pre-research project of the State Administration of Science, Technology and Industry for National Defense, China.

References

Bely, P., Laurence, R., Volonte, S., et al. 1997, Very Low Frequency Array on the Lunar Far Side, ESA report SCI (97), European Space Agency, 2

Cane, H. V. 1979, MNRAS, 189, 465

Jester, S., & Falcke, H. 2009, New Astron. Rev., 53, 1

Lindsay, J. F. 1976, Lunar Stratigraphy and Sedimentology (Amsterdam: Elsevier)

Novaco, J. C., & Brown, L. W. 1978, ApJ, 221, 114

Peragin, E., Diez, H., Darnon, F., et al. 2012, X Band downlink for CubeSat, in 26th Annual AIAA/USU Conference on Small Satellite (Logan: Utah State University), *http://digitalcommons.usu.edu/smallsat/2012/all2012/52/*

Thompson, A. R., Moran, J. M., & Swenson, G. W., Jr. 2001, Interferometry and Synthesis in Radio Astronomy (2nd edn.; New York: Wiley)

White, S. M. 2007, Asian J. Phys, 16, 189

Wilson, T. L., Rohlfs, K., & Hüttemeister, S. 2009, Tools of Radio Astronomy (5th edn., Springer-Verlag)

Woan, G. 1996, in Large Antennas in Radio Astronomy, eds. C. G. M. van't Klooster & A. van Ardenne (Noordwijk: ESTEC), 101

Woan, G. 2000, Radio Astronomy at Long Wavelengths, eds., R. G. Stone, et al. (Washington DC American Geophysical Union Geophysical Monograph Series), 119, 267

Zarka, P., Queinnec, J., Ryabov, B. P., et al. 1997, Planetary Radio Emissions IV, eds. H. O. Rucker, et al. (Wien: Austrian Acad. Sci. press), 101